Acta Biomaterialia 8 (2012) 792–801

Contents lists available at SciVerse ScienceDirect

Acta Biomaterialia

journal homepage: www.elsevier.com/locate/actabiomat

Copper-releasing, boron-containing bioactive glass-based scaffolds coated with alginate for bone tissue engineering

M.M. Erol [a], V. Mouriño [b,c,d], P. Newby [d], X. Chatzistavrou [e], J.A. Roether [f], L. Hupa [g], Aldo R. Boccaccini [d,e,*]

[a] Department of Chemical Engineering, Chemical and Metallurgical Engineering Faculty, Istanbul Technical University, Maslak 34469, Istanbul, Turkey
[b] Department of Pharmaceutical Technology, Faculty of Pharmacy and Biochemistry, University of Buenos Aires, 1113 Buenos Aires, Argentina
[c] National Science Research Council, Buenos Aires, Argentina
[d] Department of Materials, Imperial College, Prince Consort Road, London SW7 2BP, UK
[e] Institute of Biomaterials, University of Erlangen-Nuremberg, Cauerstrasse 6, 91058 Erlangen, Germany
[f] Institute of Polymer Materials, University of Erlangen-Nuremberg, Martensstrasse 7, 91058 Erlangen, Germany
[g] Process Chemistry Centre, Åbo Akademi University, Piispankatu 8, FI-20500 Turku, Finland

ARTICLE INFO

Article history:
Received 3 July 2011
Received in revised form 12 September 2011
Accepted 10 October 2011
Available online 17 October 2011

Keywords:
Bioactive glass
Scaffolds
Alginate
Cu ion release
Antibacterial

ABSTRACT

The aim of this study was to synthesize and characterize new boron-containing bioactive glass-based scaffolds coated with alginate cross-linked with copper ions. A recently developed bioactive glass powder with nominal composition (wt.%) 65 SiO_2, 15 CaO, 18.4 Na_2O, 0.1 MgO and 1.5 B_2O_3 was fabricated as porous scaffolds by the foam replica method. Scaffolds were alginate coated by dipping them in alginate solution. Scanning electron microscopy investigations indicated that the alginate effectively attached on the surface of the three-dimensional scaffolds leading to a homogeneous coating. It was confirmed that the scaffold structure remained amorphous after the sintering process and that the alginate coating improved the scaffold bioactivity and mechanical properties. Copper release studies showed that the alginate-coated scaffolds allowed controlled release of copper ions. The novel copper-releasing composite scaffolds represent promising candidates for bone regeneration.

1. Introduction

Bone tissue has a composite nature given by a highly complex and well-harmonized structure of organic and inorganic components on the microscale, macroscale and nanoscale. It is therefore not surprising that scientists are paying much attention to the development of polymer–ceramic composite materials for bone tissue engineering applications [1–3]. The relevant properties of ideal scaffolds and the requirements for their successful application in bone tissue engineering have been extensively discussed in the literature [3–5] and include excellent osteoconductivity, tailorable biodegradability, a highly interconnected porous structure, the ability to support and deliver cells, appropriate mechanical properties and the ability to fabricate irregular shapes.

Bioactive silicate glasses and glass ceramics are attractive biomaterials for bone repair and regeneration, because of their ability to enhance bone formation and to strongly bond to surrounding bone tissue in vivo [6–10]. Bioactive glasses, discovered by Hench in 1969 [11], and related silicate glass ceramics, thus constitute a group of inorganic materials highly considered in tissue engineering due to their high bioactivity [3,8,12–15]. A common characteristic of bioactive materials is the formation of an apatite-like layer on their surface when they are in contact with physiological fluids or solutions that mimic human plasma [6]. Moreover, the bioactive glass 45S5 Bioglass® (composition 45 wt.% SiO_2, 24.5 wt.% Na_2O, 24.4 wt.% CaO and 6 wt.% P_2O_5) exposes critical concentrations of Ca, Si, Na and P ions which have been shown to activate genes in osteoblast cells, thus stimulating new bone formation in vivo [16,17]. Bioactive glasses are also reported to stimulate angiogenesis [18,19]. However, 45S5 Bioglass® may have potential limitations as a scaffold material for bone repair and regeneration due to the tendency of the glass to crystallize before appreciable viscous flow during scaffold fabrication [20]. It is not possible to sinter 45S5 Bioglass® particles into a porous three-dimensional (3-D) network with adequate strength to repair bone defects and to keep the amorphous glass structure. Recently, boron-containing bioactive glasses have been developed for biomedical applications, specifically for bone tissue engineering scaffolds [21–24]. Some boron-containing bioactive glasses have been observed to undergo viscous flow sintering more readily than 45S5 Bioglass, providing a more favourable bioactive glass system for producing non-crystalline scaffolds with the relevant morphology and pore structure

* Corresponding author at: Institute of Biomaterials, University of Erlangen-Nuremberg, Cauerstrasse 6, 91058 Erlangen, Germany. Tel.: +49 0 9131 85 28601.
E-mail address: aldo.boccaccini@ww.uni-erlangen.de (A.R. Boccaccini).

1742-7061/$ - see front matter © 2011 Acta Materialia Inc. Published by Elsevier Ltd. All rights reserved.
doi:10.1016/j.actbio.2011.10.013

[24]. In addition, Gorustovich et al. [25] have found that particles of a boron-modified 45S5 Bioglass® promoted new bone formation more rapidly than standard 45S5 Bioglass® particles upon implantation into tibial defects in rats. Based on these findings, porous 3-D scaffolds based on boron-containing glasses have recently been prepared [23,24,26,27].

In recent years composites based on biopolymer-coated bioactive glass ceramic scaffolds have been developed as bone repair devices because of their high bioactivity, biocompatibility and biodegradability [28,29]. However, the need for advanced scaffold systems requires the addition of different functionalities to the substrates to be able to mimic the structure of natural bone. Functionalities such as surface reactivity, bioactivity, mechanical strength and growth factor and drug delivery capability have been considered in the design of new scaffolds with multifunctional properties [30,31]. In addition, the angiogenic and antibacterial properties of scaffolds are now being investigated in more detail, the goal being to integrate these functions in a bioactive scaffold with osteoinductive properties [32–36]. Alginate, a linear copolymer derived from various species of kelp, has useful properties, such as the ability to form gels in combination with certain metal ions, which induce cross-linking of the guluronic residues of the alginate polymer without damaging cells during the gelling process. Also, due to the biocompatibility of alginate and its simple gelation with cations such as Ca^{2+}, it is widely used for cell immobilization and encapsulation [37]. Calcium ion and ferric ion cross-linked alginates have been used in different biomedical applications such as tissue engineering scaffolds, cell encapsulation and as drug delivery systems [38]. More recently, Mouriño et al. [34] have developed Bioglass®-based scaffolds coated with sodium alginate cross-linked with Ga^{3+} for bone tissue engineering. They reported that the presence of Ga–alginate confers prophylaxis against infections. It is also known that alginate increases vascular endothelial growth factor stability and bioactivity [39]. Moreover, certain ions have an angiogenic action, promoting the development of new blood vessels, and they can also be used as antibacterial agents [40]. Angiogenesis represents an important process during the formation and repair of new tissue. Inorganic angiogenic factors, such as copper ions, are therefore of interest in the field of regenerative medicine and tissue engineering, due to their low cost, high stability and potentially greater safety compared with recombinant proteins or genetic engineering approaches [41–45]. Copper is an essential component of the angiogenic response [43]. In vivo copper release has been shown to decrease the risk of ischemia in skin flaps and to induce a vascularized capsule around a cross-linked hyaluronic acid hydrogel [44]. Barralet et al. [41] investigated the angiogenic potential of copper ions in brushite bioceramic scaffolds implanted in mice and considered the effect of low doses of copper sulphate compared with vascular endothelial growth factor (VEGF) and combinations of copper ions and VEGF. It was found that copper-loaded scaffolds not only provided directional vascularization but also enhanced wound healing. More recently, Gérard et al. [45] have studied the angiogenic and healing potential of copper ions in combination with two major angiogenic factors, VEGF and FGF-2, in a 3-D angiogenesis culture system. It was reported that the healing potential of low doses of copper ions can be applied to enhance vascularization of an implant and as alternative or complementary approach to the use of growth factors.

Based on the facts discussed above, in this work novel scaffolds were developed using a boron-containing bioactive glass which showed the desired effect of retaining an amorphous structure after sintering. The scaffolds were coated with alginate cross-linked with copper ions in order to develop for the first time bioactive silicate scaffolds with a Cu release capability for enhanced angiogenesis.

2. Materials and methods

2.1. Materials

Sodium alginate (viscosity 20–40 c.p.s., 25 °C) and cupric nitrate trihydrate ($Cu(NO_3)_2{\cdot}3H_2O$) were purchased from Sigma–Aldrich Ltd (Poole, UK). The bioactive glass powder used to fabricate the scaffolds was developed at the Process Chemistry Centre, Åbo Akademi University, Turku, Finland [46]. The nominal composition of this glass is, in wt.% 65 SiO_2, 15 CaO, 18.4 Na_2O, 0.1 MgO and 1.5 B_2O_3. The polyurethane foam (PU) (60 p.p.i.) used for scaffold fabrication by the foam replica technique [12] was obtained from Recticel Ltd (Corby, UK). All other chemicals used were of analytical grade.

2.2. Scaffold fabrication

Scaffolds were prepared using a polymer foam replication technique, as described in detail elsewhere [12]. Briefly, a 50 ml volume of slurry was prepared using 3.7 g of polyvinyl alcohol (PVA) which was dissolved in deionized water for 1 h at 80 °C. Then 15 g of glass powder were dispersed in the solution under constant stirring. This glass powder concentration in the slurry was found, by a simple trial-and-error approach, to lead to a suitable slurry viscosity for fabrication of scaffolds by the foam replica method. A polyurethane foam with a structure comparable with that of human trabecular bone was used as a sacrificial template for the replication method. The foam was cut into $10 \times 10 \times 10$ mm samples.

Foams were immersed in the slurry for 3 min so that the foam struts were coated with bioactive glass particles. The as-coated foams were then dried at room temperature overnight and then subjected to a controlled heat treatment. The samples were heated at 2 K min^{-1} to 550 °C in air to decompose the foam, then at 2 K min^{-1} to 650 °C, at which temperature they were kept for 4 h to densify the glass network without crystallizing the glass. The scaffolds were then coated with sodium alginate cross-linked with copper following a procedure described elsewhere [34]. Several preliminary experimental trials were carried out in order to control the amount of copper loaded. Controlling the viscosity of the alginate solution cross-linked with copper is required, since the quality of the coating depends on it. In addition, the alginate solution should not block the pores of the scaffold. It was observed that alginate viscosity increased with increasing copper concentration. Taking into account the total amount of copper that the scaffolds were able to absorb and the need to achieve a suitable alginate viscosity, three different concentrations of Cu^{2+} (in water) were used: 0.5, 5 and 10 mg ml^{-1}. In all cases the copper solution was added dropwise to the scaffolds with the help of a syringe and the loaded scaffolds were left to dry for 1 h at 37 °C. The amount of solution loaded to the scaffold was estimated from the difference in weight of the syringe. Then sodium alginate in water (1 wt.%) was added dropwise to the scaffolds, which were left to dry at 37 °C for 1 h and subsequently at room temperature overnight for cross-linking by the copper ions. Coated and uncoated scaffolds were coded 05S, 5S, 10S and GS, corresponding to scaffolds coated with sodium alginate cross-linked with 0.5, 5 or 10 mg ml^{-1} Cu^{2+} and untreated scaffold, respectively.

2.3. Characterization

2.3.1. Thermal analysis

Differential thermal analysis (DTA) was performed on the glass powder using a TGA/SDTA851e instrument from Mettler Toledo, at a heating rate of 20 K min^{-1} up to 1200 °C. Sintering and crystallization of the glass powder were also investigated by hot stage

microscopy (HSM) (Misura 3.0, Expert Systems) using a heating rate of 5 K min^{-1} up to 1200 °C. The shrinkage behaviour was studied by in situ measurement of specimen height as a function of temperature by HSM.

2.3.2. Porosity

The porosities of the uncoated (P_1) and coated (P_2) scaffolds were determined applying the equations

$$P_1 = 1 - (W_1/\rho_1 V)$$

$$P_2 = 1 - ([(W_1/\rho_1) + (W_2 - W_1/\rho_1)]/V)$$

where W_1 is the weight of the uncoated scaffold, W_2 is the weight of the coated scaffold, V is the volume of the scaffold, ρ_1 is the density of the bioactive glass (2.37 g cm^{-3}) and ρ_2 is the density of the coating material (0.992 g cm^{-3}).

2.3.3. Surface morphology

Scanning electron microscopy (SEM) with energy dispersive spectroscopy (EDS) (JEOL 5610L and JEOL JSM-6400) was used for the morphological and elementary characterization of coated and uncoated scaffolds. Samples were fixed on a SEM sample holder, air dried under vacuum and coated with a thin layer of gold.

2.3.4. Structural analysis

X-ray diffraction (XRD) analysis of the coated and uncoated 3-D scaffolds was performed using Philips PW 1700 and PANalytical X'Pert Pro diffractometers to investigate the characteristic phases and possible crystallinity of the fabricated samples. Data were obtained over the range 2 = 10–80° using a step size of 0.04° and counting time of 25 s per step employing CuK_α radiation (at 40 kV and 40 mA). FTIR spectra were collected using a Perkin–Elmer Multiscope spectrometer in transmittance mode in the mid infrared region (4000–400 cm^{-1}). All samples were characterized before and after immersion in simulated body fluid (SBF) (see below). For XRD and FTIR measurements the samples were ground and measured in powder form.

2.3.5. Mechanical properties

The compressive strength of prismatic samples (dimensions 5 × 5 × 10 mm) was measured using a Zwick/Roell Z010 servo-hydraulic testing instrument. The cross-head speed was 0.5 mm min^{-1} with a pre-load of 1 kN. At least five specimens for each sample series were tested. Average values and standard deviations were determined.

2.3.6. Assessment of bioactivity

The acellular bioactive behaviour of the scaffolds was determined in vitro through immersion of samples in SBF, as described by Kokubo et al. [47]. Each 5 × 5 × 5 mm sample was immersed in 30 ml of SBF and stored in an incubator at a temperature of 37 °C. Samples were immersed in SBF for different periods: 1, 3, 5, 7, 14 and 28 days. When samples were removed from the SBF solution they were rinsed with ethanol and water, and dried at 37 °C for 30 min. The samples were then characterized using SEM, XRD and FTIR.

2.3.7. Water uptake and weight loss measurements

Water absorption (%W_A) and weight loss (%W_L) of the samples upon immersion in SBF were determined over the 28 day period using the equations:

$$\%W_A = ((W_{t,wet} - W_{t,dry}/W_{0,dry})/ \times 100$$

$$\%W_L = ((W_{0,dry} - W_{t,dry})/W_{0,dry}) \times 100$$

where $W_{0,dry}$ is the original sample weight measured before immersion in SBF. To measure the water absorption (%W_A) immersed samples were removed at given time points, gently wiped and weighed ($W_{t,wet}$). Similarly, to measure the weight loss (%W_L) the samples were removed from the SBF solution, dried at 37 °C overnight and subsequently weighed ($W_{t,dry}$).

2.3.8. Copper release investigation

Changes in the concentration of copper in the SBF solution as a result of soaking the scaffolds for 1, 3, 5, 7, 14 and 28 days were measured using inductively coupled plasma optical emission spectrometry (ICP-OES). A Perkin Elmer Model Optima 2100 ICP operated at 13.56 MHz (using Ar and N_2 gases) was used for the measurements.

3. Results and discussion

3.1. Thermal analysis and heat treatment

Fig. 1 shows the results of the DTA and HSM experiments. It can be seen from Fig. 1 that there is one endothermic peak at 608 °C, indicating the glass transition. Sintering of the glass shows a shallow exothermic peak in the temperature range 708–808 °C. The second exothermic peak indicating crystallization starts at around 800 °C and has a maximum value at around 872 °C. This type of glass, for which sintering and crystallization partly overlap (as is the case for 45S5 Bioglass®), exhibit a strong peak indicating both crystallization and sintering, which is usually seen slightly above the glass transition, followed by a smaller peak (in this case at ~1050 °C) indicating other crystals precipitating, liquidus formation, etc. The endothermic peak identified in the DTA curve at ~1100 °C is related to melting of the crystals. As can be seen from the HSM curve, there are three characteristic steps. The first starts at around 660 °C, representing sintering through viscous flow. The second is between 810 and 1000 °C and is related to crystallization. The last step at a higher temperature is attributed to melting of the crystals, in agreement with the DTA results. The sharp decrease in sample height interferes with the viscosity of the residual glassy phase between the crystals. Several preliminary experimental trials were conducted at different temperatures and residence times in order to determine the optimum sintering conditions for the fabrication of 3-D scaffolds from bioactive glasses by the foam replica method. The sintering temperature and the residence time, which were selected on the basis of preliminary runs, were 600–700 °C and 2–4 h, respectively. The foams were sintered at four different temperatures to determine the lowest possible sintering

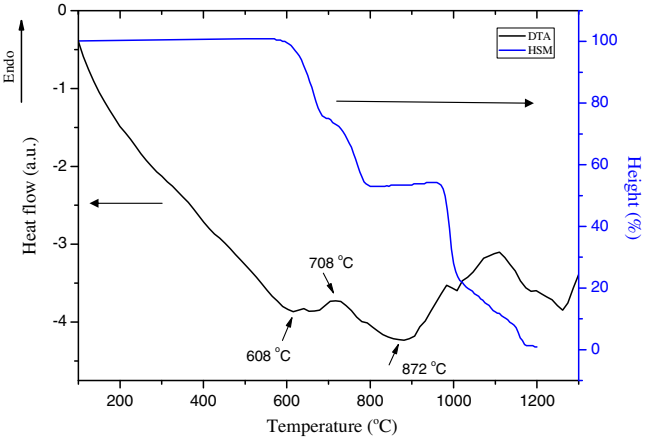

Fig. 1. Thermal behaviour of the bioactive glass from DTA and HSM measurements.

temperature. On the basis of preliminary experimental trials an optimum sintering temperature of 650 °C and a holding time of 4 h were found to be appropriate for the fabrication of scaffolds with adequate porosity, pore size and mechanical properties.

3.2. Microstructural characterization

Visual inspection of the scaffolds obtained confirmed that they maintained their prismatic form without significant distortion despite the considerable (isotropic) shrinkage of the macrostructure. The shrinkage in volume of the scaffolds after sintering at 650 °C was about 50%. It was observed that the samples preserved their initial shape, without collapsing the macroporous structure. The macroporous network and the strut microstructure of the coated and uncoated scaffolds are illustrated in Fig. 2. As can be seen from these figures, highly porous scaffolds with interconnected porosity were produced. Similar morphologies have been reported for a variety of sintered foams synthesized by the foam replica method [12,15,26]. Inspection of the SEM images indicates that alginate has attached to the bioactive glass scaffold surface forming a uniform coating without blockage of the pores, as observed in Fig. 2c and d. It can be observed that the interconnected porosity is also maintained after polymer coating. The porosities of the coated and uncoated scaffolds are 82 ± 2% and 79 ± 2%, respectively. The average pore size of the coated scaffolds was found to be 325 μm, with pore size variations in the range 110–550 μm, which is in the size range desired for application as a bone tissue engineering scaffold [3–5].

The strut microstructure can be seen in Fig. 2b and d. The typical hollow centre, which is common in scaffolds fabricated by the foam replica method [12], is not visible. This is a significant result regarding achieving improved mechanical properties of the scaffolds. The microstructure of the sintered struts indicates that significant sintering had occurred and this result confirms that the sintering parameters had been correctly chosen, leading to densification by viscous flow without the macroporous structure collapsing. This rather dense structure of the struts should lead to favourable mechanical properties, as discussed further below. It can be also observed in Fig. 2d that the alginate coating covered the surface of the struts fairly uniformly and the glass strut surface morphology is not clearly visible, which indicates a homogeneous distribution of the polymer coating on the surface of the scaffold. Thus the SEM observations confirm that the interconnected character of the porosity and the pore size of the scaffolds coated with alginate cross-linked with copper are suitable for the intended application, e.g. are favourable for cell attachment, migration and vascularization [48,49].

3.3. Mechanical behaviour

The compressive strengths of the uncoated and coated scaffolds are shown in Fig. 3. As can be seen, the compressive strength of the scaffolds was increased by coating with alginate cross-linked with copper ions when with uncoated scaffolds. It is suggested that the alginate layer covers the struts and fills microcracks on the strut surface, improving the mechanical stability of the scaffold. This is in agreement with what is known in the field of polymer-coated porous ceramics [28,29] and also as investigated in our previous study [34]. The measured compressive strength values, in the range 0.6–1 MPa, fall close to the lower bound of the values for spongy bone. The highest mean compressive strength (1.0 ± 0.3 MPa) was obtained for the 10S sample. The potential to improve the mechanical properties of scaffolds based on polymer-coated bioceramics has been demonstrated in several systems [28,29,50–52], which have achieved mechanical properties, in particular compressive strength, in the range of values typical of cancellous bone. For example, coating 45S5 Bioglass®-derived scaffolds with poly(3-hydroxybutyrate) (PHB) resulted in a considerable increase in the compressive strength of the scaffolds (1.5 MPa at 85% porosity) [52]. According to previous experience with these materials [52] the compressive strength achieved with these scaffolds is sufficient for the scaffolds to be handled safely in the laboratory and for effective manipulation for in vivo studies. A similar result was recently reported by Mouriño et al. [34], who developed Bioglass®-derived glass ceramic scaffolds coated with alginate. However, the highest measured compressive strength of scaffolds with 89–92% porosity was 0.79 MPa, which is lower than the values obtained in this study. In addition, the present results indicate that the compressive strength values increased with copper content. This result could be attributed to increased cross-linking density, however, this suggestion has not been proven. Kuo and

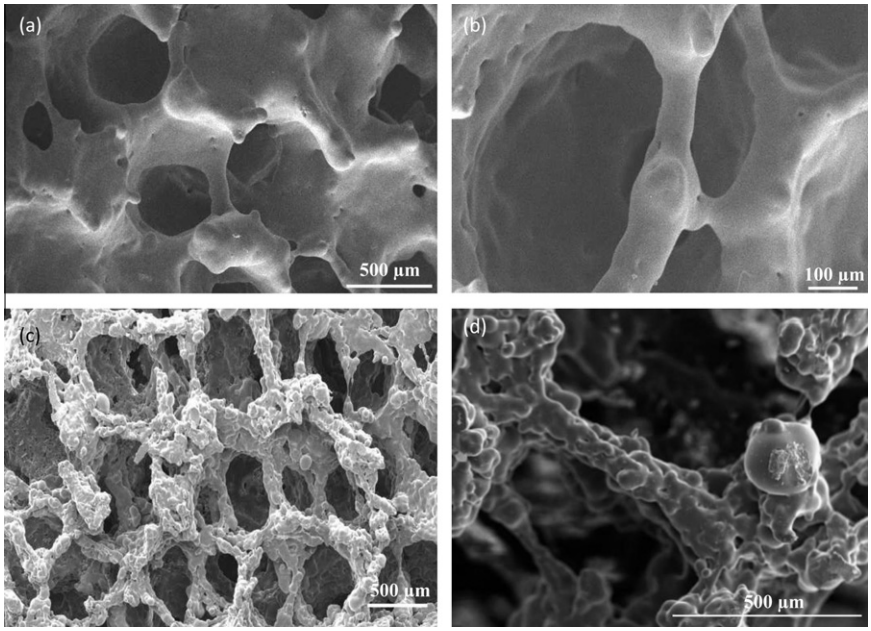

Fig. 2. SEM images showing typical (a) pore and (b) strut microstructures of a scaffold sintered at 650 °C for 4 h and of an alginate-coated scaffold (sample 10S) at (c) low and (d) high magnification. These are representative images of the scaffold cross-sections. Similar results were obtained for the 05S and 5S scaffolds.

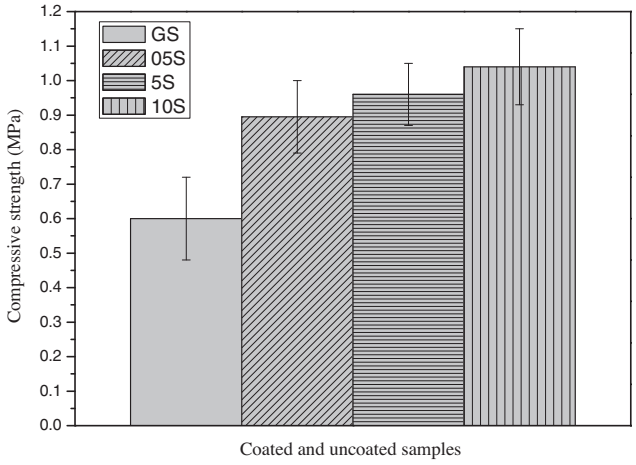

Fig. 3. Compressive strength values of alginate-coated (05S, 5S and 10S) and uncoated (GS) scaffolds.

Ma [53,54], working with Ca^{2+} as the cross-linking ion, found that higher calcium contents resulted in improved mechanical properties of homogeneous alginate gels. It was found that a decrease in calcium content results in a decrease in mechanical properties due to a lower cross-link density and polymer concentration. It remains to be investigated whether or not a similar mechanism is active in Cu cross-linked alginate, which is the focus of the current study.

3.4. Structural analysis

The transmittance spectra of both uncoated (GS) and 05S coated scaffolds are shown in Fig. 4a. The characteristic GS spectrum exhibits a peak at ~590 cm^{-1} assigned to the Si–O bending mode, and the characteristic peak of the modified silicate network is seen at ~800 cm^{-1} [55]. The respective spectrum of the 05S sample indicates all the features assigned to the glass network. Furthermore, there are some additional shallow peaks in the range 1500–1760 cm^{-1}, which can be assigned to the absorption bands of asymmetric and symmetric stretching vibration of carboxylate ions of sodium alginate, while the major peaks at ~2900 cm^{-1} and in the range 3150–3450 cm^{-1} are attributed to the C–H and unsaturated asymmetric O–H stretching vibrations, respectively [34,56].

The XRD pattern of the uncoated scaffold shown in Fig. 4b indicates the amorphous state of the bioactive glass after sintering. To achieve a scaffold with amorphous structure is an important result, considering that most common bioactive glasses crystallize during the sintering process [20] and usually sintered scaffolds made from bioactive glass powders exhibit different degrees of crystallinity [12]. An amorphous phase can be thermodynamically less stable than its crystalline counterpart, which is expected to result in enhanced dissolution behaviour and higher bioactivity in comparison with partially crystallized scaffolds. The XRD pattern of alginate-coated scaffolds (e.g. scaffold 10S) indicates that the amorphous structure is retained after coating (Fig. 4b). Moreover, the XRD results suggest that copper only reacted with alginate, since there was no indication of the presence of metallic copper or copper oxide in the XRD pattern of scaffold 10S. These results are also in agreement with previous data on Bioglass®-derived glass ceramic scaffolds coated with alginate cross-linked with gallium [34].

3.5. Degradation behaviour

The scaffold degradation rate is a critical design parameter for bone tissue regeneration because appropriate scaffold degradation

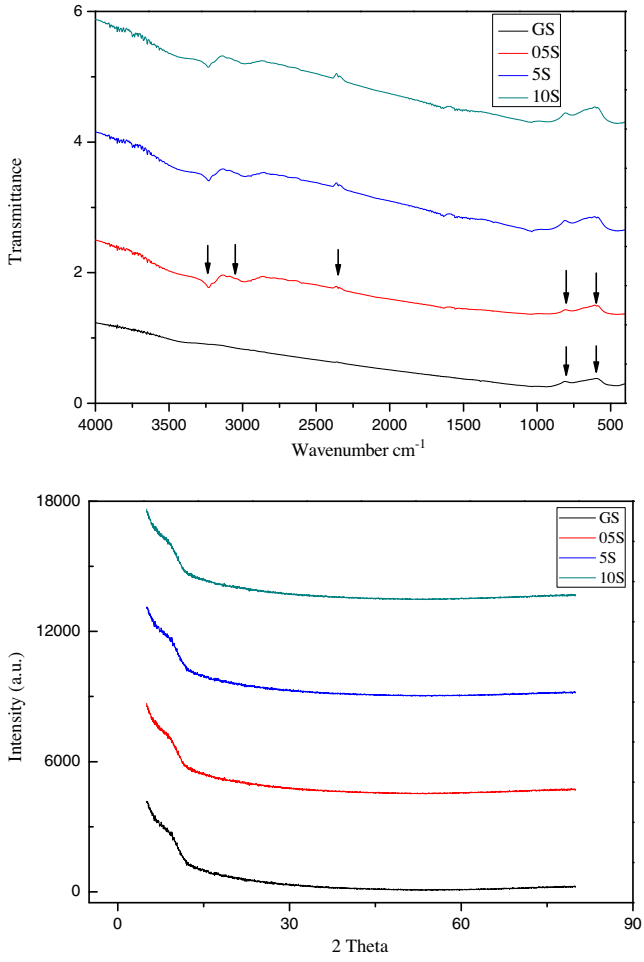

Fig. 4. (a) FT-R spectra and (b) XRD patterns of uncoated and alginate-coated (10S) samples. Similar results were obtained for the 05S and 5S scaffolds.

provides the space for matrix deposition and tissue growth, which may ultimately lead to improved quantity and quality of regenerated bone [57]. In this study the degradation of coated and uncoated scaffolds was monitored by water absorption, weight loss, and pH variation in SBF. Fig. 5a shows the water absorption results. It is seen that after 1 day immersion in SBF all samples exhibit considerable water uptake values due mostly to filling of the pores with water. Compared with the uncoated scaffolds, the rate of water absorption was remarkably increased in the coated scaffolds. It has been reported that alginate absorbs water quickly and is capable of absorbing 200–300 times its own weight [37]. A high water absorption capability of alginate-coated scaffolds was observed in this study. However, no significant difference could be seen in the trends among the three types of coated scaffolds investigated here as the amount of sodium alginate used in all cases was the same.

The weight loss of the composite scaffolds is shown in Fig. 5b. The weight loss is seen to increase with immersion time and varies with the type of alginate coating. The degradation of alginate can be controlled by varying the alginate molecular weight and chemical structure, and by cross-linking [58]. Although alginates are hydrophilic and water-soluble anionic polysaccharides, cross-linking with cationic ions leads to a sufficiently stable material in aqueous media [59]. In the context of the present alginate coatings it is ion exchange involving Cu^{2+} ions which is responsible for the swelling and subsequent degradation of the alginate. Na^{+} ions present in the SBF solution could undergo ion exchange with Cu^{2+} ions which bind $-COO^{-}$ groups in alginate. Since Na^{+} ions are unable to efficiently

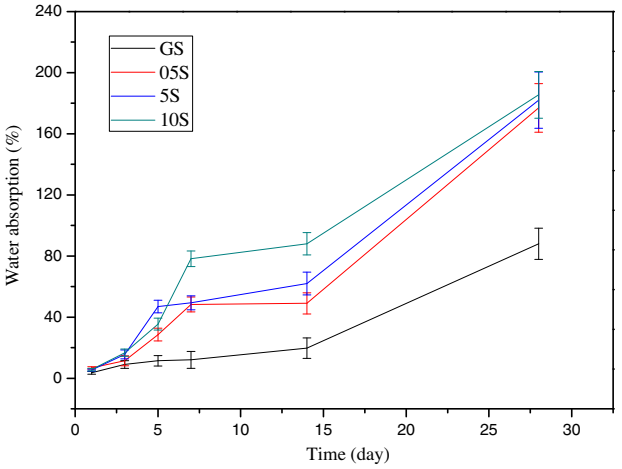

(a)

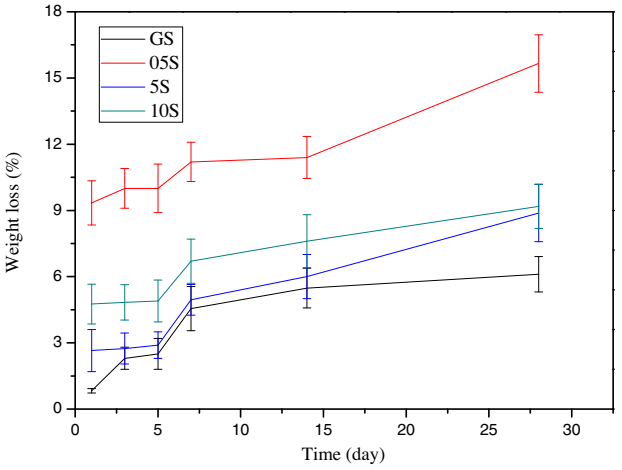

(b)

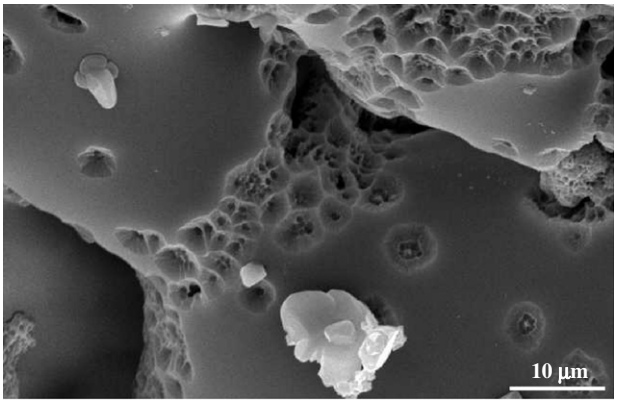

(c)

Fig. 5. (a) Water absorption and (b) weight loss values for alginate-coated (05S, 5S and 10S) and uncoated (GS) scaffolds. (c) SEM micrograph of an uncoated scaffold after immersion in SBF for 1 day showing surface degradation of the glass.

bind $–COO^-$ ion groups in alginate the extent of cross-linking decreases and, hence, water uptake and weight loss increase. The number and rate of cationic ions diffusing out from the alginate depend upon the Na^+ concentration in the SBF solution [59,60]. Bajpai and Sharma [59] studied the degradation behaviour of alginate cross-linked with Ca^{2+} in both NaCl solution and distilled water and it was found that alginate only degraded in NaCl solution. It was reported that ion exchange between Na^+ ions binding carboxylate groups in alginate is ultimately responsible for the swelling and subsequent degradation of the alginate [59]. Weight loss of the coated scaffolds resulted not only from degradation of the alginate coating but also from dissolution of the glass during immersion in SBF, considering also the in situ growth of hydroxyapatite (HA) crystals on scaffold surfaces when immersed in SBF (see also Section 3.6). Fig. 5c shows a SEM micrograph of an uncoated scaffold after immersion in SBF for 1 day. The presence of small cavities on the glass surface can be observed, which is evidence of surface degradation of the glass. These pores indicate dissolution of the glass matrix in the early stages of SBF immersion. It was also observed (Fig. 5b) that weight loss of the 05S sample is higher than that of the other coated scaffolds. This result may be explained by considering the copper content in the alginate. In aqueous medium sodium alginate behaves like an anionic polymer due to the presence of negatively charged $–COO^-$ groups. Since copper ions are divalent, bonding to alginate is expected to occur in a planar two-dimensional manner inside the alginate molecule [60]. Cross-linking should occur in two different planes, resulting in compaction of the alginate molecules. Extended two-dimensional cross-linking will lead to greater alginate stability [59]. Due to the higher concentration of copper, more divalent cations can be captured inside the matrix, which should play a significant role in bridging the gel network. This explains why the 05S sample weight loss is higher than that of the 5S and 10S samples.

The pH of the SBF medium in which the uncoated scaffolds were immersed varied in the range 7.19–7.78, while the pH of the medium of coated ones varied in the range 7.35–7.83. The pH of the medium was almost stable during the immersion studies, with the acidic groups resulting from the degradation of alginate decreasing the pH while calcium and silicate ions from dissolution of the glass surface compensate for this pH decrease. Thus, the pH of the medium depends on both the degradation rate of the polymer and the dissolution profile of the glass, as discussed in the literature [61]. It should also be noted that the degradation behaviour of alginate can be controlled at pH 7.4 [62], a value that falls in the pH range measured in this study.

3.6. Bioactivity assessment

The response of 3-D composite scaffolds in contact with SBF was analyzed using SEM-EDS, XRD and FTIR. Fig. 6 shows XRD patterns indicating the gradual development of a HA layer on the surface of uncoated scaffolds following increasing time of immersion in SBF. As seen in Fig. 6, small peaks at 32° 2θ and between 47° and 49° 2θ were detected in XRD patterns of samples soaked in SBF for 7 and 14 days. These peaks can be assigned to HA ($Ca_{10}(PO_4)_6(OH)_2$) according to the standard JCPDS cards (09-4-0432). The XRD patterns given in Fig. 6a also confirm the amorphous structure of the bioactive glass scaffold before and after immersion in SBF for 1–7 days. It is apparent that an HA layer formed on the surface of the bioactive glass scaffold after 7 days in SBF. The results were compared with those obtained for coated scaffolds (Fig. 6b), which were also immersed in SBF for varying times. Four peaks corresponding to HA were detected, as shown in Fig. 6b, confirming that a HA layer had formed on the surface of the coated scaffolds by the third day of immersion in SBF. It is apparent that the rate of HA formation on coated scaffolds was faster than on uncoated scaffolds. This indicates higher bioactivity of the coated scaffolds, which can be attributed to the bioactive behaviour of alginate, as discussed below.

FTIR spectra of both uncoated and coated scaffolds after immersion in SBF for 1, 3, 5, 7 and 14 days are presented in Fig. 7. The FTIR spectra of uncoated scaffolds do not show any significant difference until 14 days immersion in SBF. After 14 days immersion

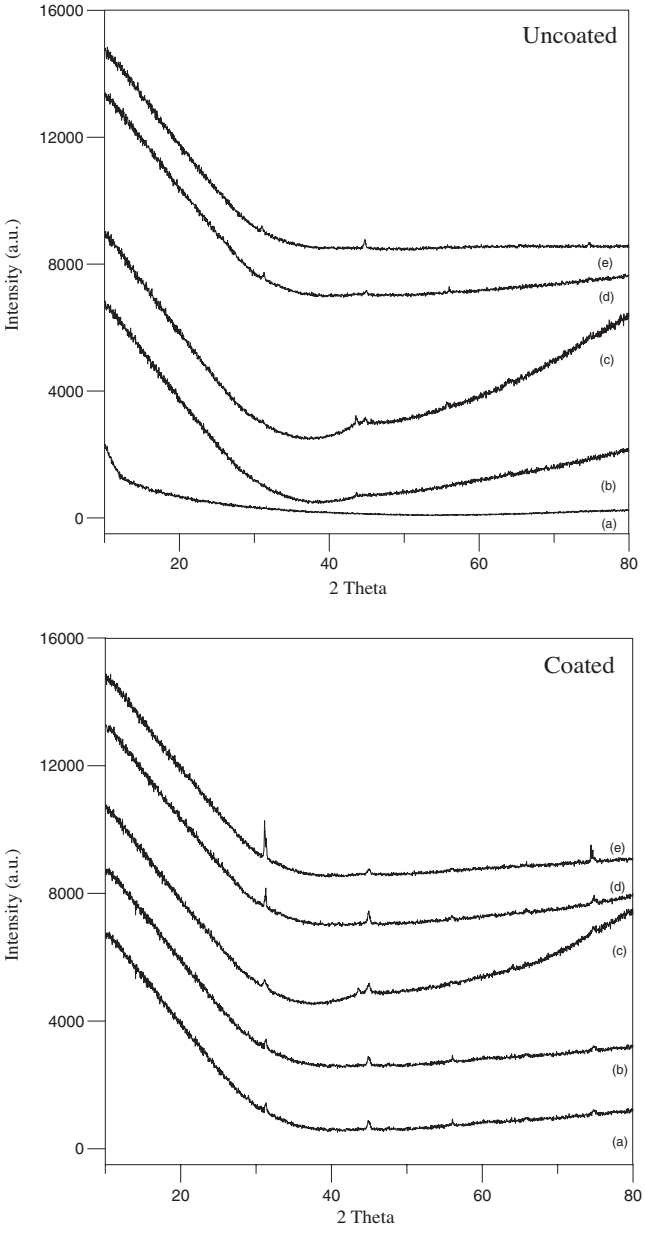

Fig. 6. XRD patterns of uncoated (GS) and alginate-coated (05S) scaffolds after (a) 1, (b) 3, (c) 5, (d) 7 and (e) 14 days immersion in SBF. Similar results were obtained for the 5S and 10S scaffolds.

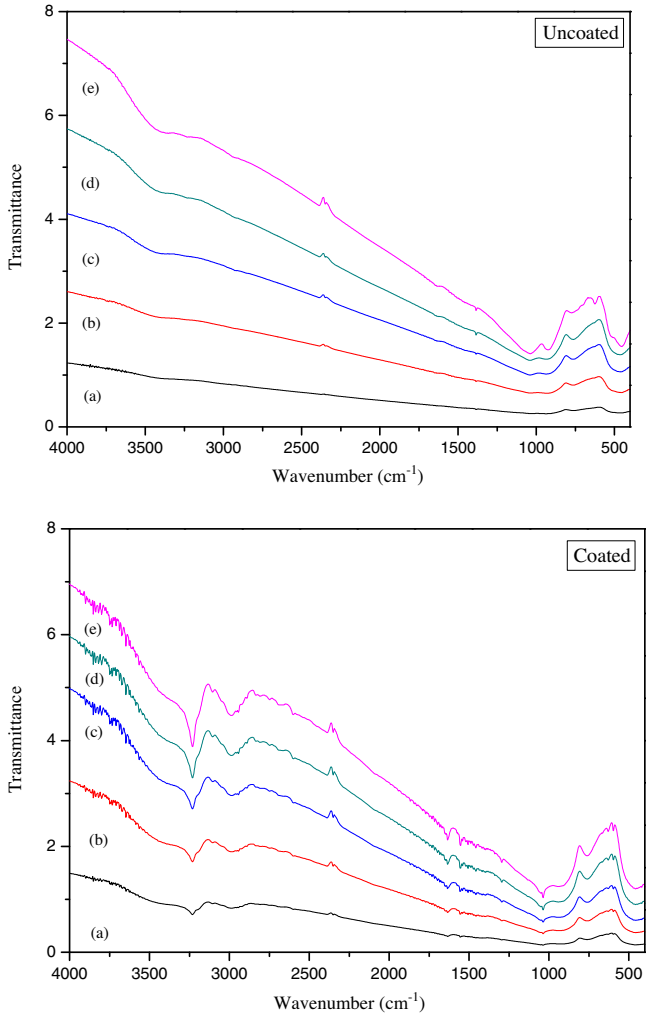

Fig. 7. FTIR spectra of uncoated (GS) and alginate-coated (05S) scaffolds after (a) 1, (b) 3, (c) 5, (d) 7 and (e) 14 days immersion in SBF. Similar results were obtained for the 5S and 10S scaffolds.

there are two small peaks at ~575 and 600 cm^{-1} and a slight shift of the peak at ~1030 cm^{-1}, which can be attributed to the deposition of calcium and phosphate groups that had started to occur. The FTIR spectra of the coated scaffolds also exhibit similar peaks corresponding to calcium and phosphate groups. These peaks are visible after only 3 days immersion in SBF. With increasing immersion time the characteristic peaks of the HA phase become slightly sharper, indicating an increase in crystallinity. Thus FTIR characterization confirms that the coated scaffolds exhibit rapid formation of HA compared with uncoated scaffolds. It has been reported that alginate shows bioactive behaviour in in vitro SBF studies [63]. This effect can explain the improved bioactivity of alginate-coated scaffolds compared with that of uncoated scaffolds in our study.

Fig. 8a shows a SEM micrograph of an uncoated scaffold after 7 days immersion in SBF. It is apparent that HA crystals are formed as a result of contact of the bioactive glass struts with SBF. Crystalline structures were also observed on the strut surfaces of the coated scaffold after 7 days in SBF, as shown in Fig. 8b. The formation of HA on the surfaces of the coated and uncoated scaffolds after immersion in SBF was confirmed by EDX analysis (shown in Fig. 8). High Ca and P peaks from HA were detected. The process of HA formation is based on ion exchange between the scaffold surface and the SBF solution, which is the well-known mechanism proposed for bioactive glasses by Hench [6]. In the first stage a silica-rich layer is formed on the scaffold surface, followed by nucleation and growth of HA crystals on top of this silica-rich layer. However, as can be seen in Fig. 8b, HA crystals also formed on the surface of the alginate in the present polymer-coated scaffolds. This can be explained by considering ion exchange between the alginate and SBF medium. It is known that ionically cross-linked alginate has a tendency to swell and eventually dissolve in tissue culture medium, SBF and other biological solutions. This phenomenon has been demonstrated by a number of studies characterizing swelling [53,54]. It is suggested that copper ions diffuse out of the alginate matrix, leading to greater water uptake and faster degradation of the coating. In addition, possible disruption of the alginate coating leading to direct contact between the bioactive glass surface and SBF cannot be ruled out. This may facilitate the precipitation of calcium phosphate on this structure. As can be observed in Fig. 8b, there were small voids in the polymer coating which are evidence of opening of the alginate structure. It should also be noted that high Ca and P peaks from HA were detected by EDX

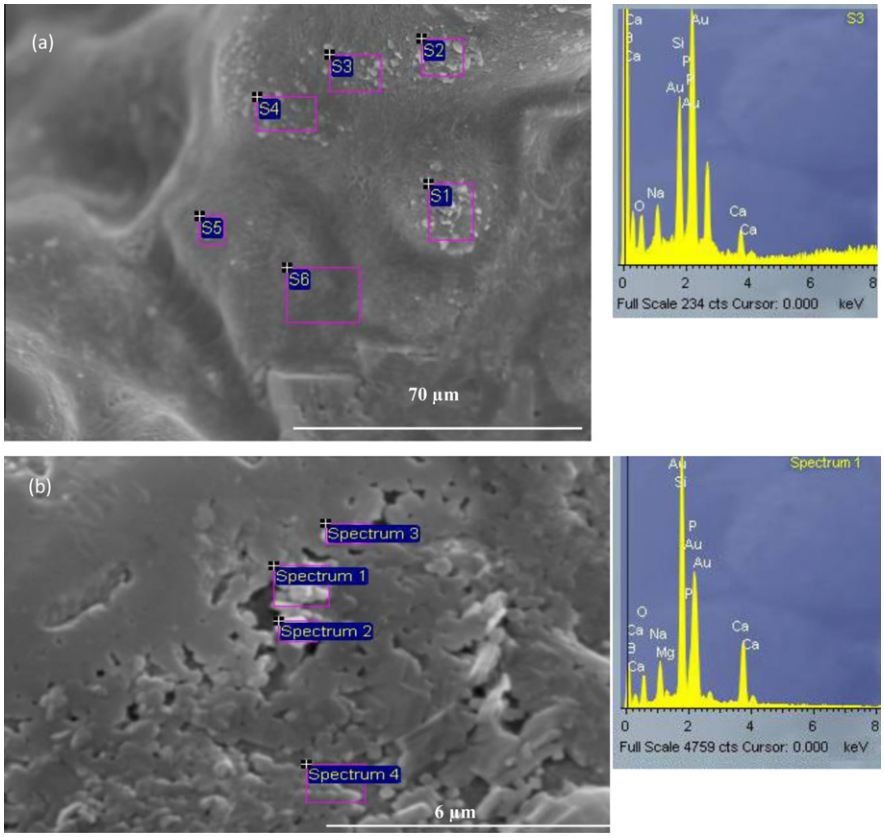

Fig. 8. SEM images showing the surface of (a) uncoated and (b) alginate-coated (10S) scaffolds after 7 days immersion in SBF, with EDS results on a selected area of the samples. Similar results were obtained for the 05S and 5S scaffolds.

analysis especially in these regions. Thus the rapid degradation and bioactive behaviour of alginate contributes to a faster HA formation rate on the coated scaffolds than on the uncoated ones.

3.7. Copper release

Copper release from the alginate-coated scaffolds was determined in order to correlate ion exchange with the swelling and degradation profile of the alginate. Fig. 9 shows that the number of Cu^{2+} ions released from the scaffolds increases with increasing immersion time. This can be attributed to the degradation of alginate based on an ion exchange process involving Cu^{2+}, described above. The faster release of copper for scaffold 10S can be explained based on the high concentration of copper in it. Several studies in the literature provide evidence of the marked effect of Cu ions on cells and bacteria. Kim et al. [64] produced Cu^{2+}-containing HA (Cu/HA) and reported that it exhibited a strong antibacterial effect on *Esherichia coli* and *Staphylococcus aureus*. Sutter et al. [65] investigated the properties of Cu/HA crystals and results showed that Cu/HA has a lower dissolution rate than pure HA. However, it was also reported that the higher concentration of Cu ions on the surface of HA nanoparticles allows faster diffusion of toxic Cu ions to the surrounding medium, penetrating and killing bacterial cells [66]. Varmette et al. [67] showed that Cu-containing glasses had no therapeutic effect due to a toxic Cu level (58 p.p.m.) released into the culture medium. In related studies Singh et al. [68] reported that the cell proliferation rate decreased with increasing copper concentration. It is therefore clear that a possible burst release and a higher concentration of copper could be cytotoxic and provide unfavourable conditions for cell attachment and growth. Thus it is proposed that the slow release of

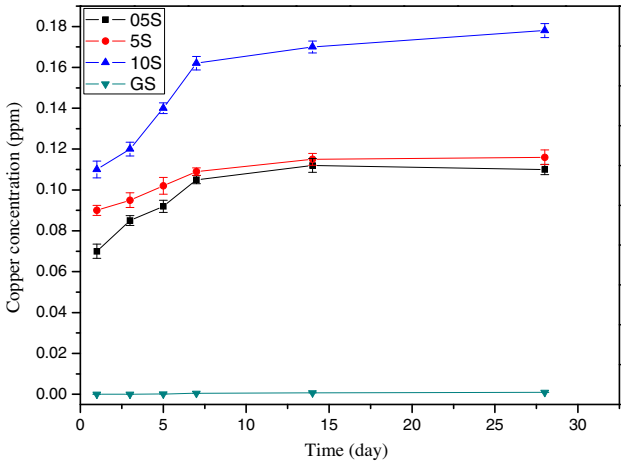

Fig. 9. Copper ion release from alginate-coated scaffolds loaded with different amounts of copper as a function of immersion time in SBF.

copper, as observed in scaffolds 05S and 5S, is favourable for possible tissue engineering applications of the present scaffolds. Barralet et al. [41] investigated the angiogenic potential of copper ions in brushite ceramic scaffolds implanted in mice and the effect of low doses of copper sulphate compared with VEGF and combinations of copper ions and VEGF. It was reported that low doses of copper sulphate (0.56 mg ml^{-1}) optimized angiogenesis during tissue ingrowth, whereas a 10-fold increase in the dose (i.e. 5.6 mg ml^{-1}) enhanced wound tissue in-growth. Thus the copper content within the alginate coatings in the present study (especially the 05S and

5S scaffolds) should be sufficient to promote the angiogenic potential of the present glass-derived composite scaffolds.

4. Conclusions

Biodegradable and mechanically robust non-crystalline bioactive glass scaffolds have been successfully synthesized by the replication technique using a boron-containing silicate glass. The scaffolds were coated with sodium alginate cross-linked with Cu. The compressive strength of the alginate-coated scaffolds was found to be higher than that of the uncoated scaffold. The coated scaffolds were seen to exhibit improved bioactive behaviour compared with the uncoated one. Copper release studies indicated that the new scaffolds showed controlled release of copper ions, which could be beneficial in promoting the angiogenic potential of the scaffolds for bone regeneration. For tissue engineering applications cell attachment, migration and vascularization are all important considerations. The controlled release of boron and copper from the present scaffolds will be investigated in the context of the emerging field of bioactive glasses with therapeutic ion release capabilities [40]. Future efforts will be focused on in vitro and in vivo studies to investigate the performance of these functional scaffolds under conditions relevant to applications in bone tissue engineering.

Acknowledgement

M.M.E. gratefully acknowledges financial support from The Scientific and Technological Research Council of Turkey.

Appendix A. Figures with essential colour discrimination

Certain figures in this article, particularly Figs. 1, 4, 5, 7–9, are difficult to interpret in black and white. The full colour images can be found in the on-line version, at doi:10.1016/j.actbio.2011.10.013).

References

[1] Wei G, Ma PX. Polymer/ceramic composite scaffolds for bone tissue engineering. In: Ma PX, Elisseeff J, editors. Scaffolding in tissue engineering. Boca Raton, FL: CRC Press; 2006. p. 241–52.
[2] Wang M. Composite scaffolds for bone tissue engineering. Am J Biochem Biotechnol 2006;2:80–4.
[3] Rezwan K, Chen QZ, Blaker JJ, Boccaccini AR. Biodegradable and bioactive porous polymer/inorganic composite scaffolds for bone tissue engineering. Biomaterials 2006;27:3413–31.
[4] Guarino V, Causa F, Ambrosio L. Bioactive scaffolds for bone and ligament tissue. Exp Rev Med Devices 2007;4:405–18.
[5] Hutmacher DW. Scaffold design and fabrication technologies for engineering tissues – state of the art and future perspectives. J Biomater Sci Polym E 2001;12:107–24.
[6] Hench LL. Bioceramics. J Am Ceram Soc 1998;81:1705–28.
[7] Vrouwenvelder WCA, Groot CG, de Groot K. Better histology and biochemistry for osteoblasts cultured on titanium-doped bioactive glass: Bioglass 45S5 compared with iron, titanium, fluorine and boron-containing bioactive glasses. Biomater 1994;15:97–106.
[8] Hench LL, Thompson I. Twenty-first century challenges for biomaterials. J Roy Soc Interface 2010;7:S379–91.
[9] Yao J, Radin S, Leboy S, Ducheyne P. The effect of bioactive glass content on synthesis and bioactivity of composite poly(lactic-co-glycolic acid)/bioactive glass substrate for tissue engineering. Biomaterials 2005;26:1935–45.
[10] Hupa L, Karlsson KH, Hupa M, Aro HT. Comparison of bioactive glasses in vitro and in vivo. J Biomed Mater Res B 2010;93:573–80.
[11] Hench LL, Splinter RJ, Allen WC, Greenlee TK. Bonding mechanisms at the interface of ceramic prosthetic materials. J Biomed Mater Res 1971;2:117–41.
[12] Chen QZ, Thompson ID, Boccaccini AR. 45S5 Bioglass®-derived glass-ceramic scaffolds for bone tissue engineering. Biomater 2006;27:2414–25.
[13] Vitale-Brovarone C, Verne E, Robiglio L, Appendino P, Bassi F, Martinasso G, et al. Development of glass-ceramic scaffolds for bone tissue engineering: characterisation, proliferation of human osteoblasts and nodule formation. Acta Biomater 2007;3:199–208.
[14] Livingston T, Ducheyne P, Garino JJ. In vivo evaluation of a bioactive scaffold for bone tissue engineering. Biomed Mater Res 2002;62:1–13.
[15] Baino F, Vitale-Brovarone C. Three-dimensional glass-derived scaffolds for bone tissue engineering: current trends and forecasts for the future. J Biomed Mater Res A 2011;97:514–35.
[16] Hench LL. Genetic design of bioactive glass. J Eur Ceram Soc 2009;29:1257–65.
[17] Xynos ID, Edgar AJ, Buttery LDK, Hench LL, Polak JM. Gene-expression profiling of human osteoblasts following treatment with the ionic products of Bioglass® 45S5 dissolution. J Biomed Mater Res 2001;55:151–7.
[18] Leach KJ, Kaigler D, Wang Z, Krebsbach PH, Mooney DJ. Coating of VEGF-releasing scaffolds with bioactive glass for angiogenesis and bone regeneration. Biomater 2006;27:3249–55.
[19] Gorustovich AA, Roether JA, Boccaccini AR. Effect of bioactive glasses on angiogenesis: a review of in vitro and in vivo evidences. Tissue Eng B 2010;16:199–207.
[20] Bretcanu O, Chatzistavrou X, Paraskevopoulos K, Conradt R, Thompson I, Boccaccini AR. Sintering and crystallisation of 45S5 Bioglass® powder. J Euro Ceram Soc 2009;29:3299–306.
[21] Fu Q, Rahaman MN, Fu H, Liu X. Silicate, borosilicate, and borate bioactive glass scaffolds with controllable degradation rate for bone tissue engineering applications. I. Preparation and in vitro degradation. J Biomed Mater Res A 2010;95(1):164–71.
[22] Day DE, White JE, Brown RF, McMenamin KD. Transformation of borate glasses into biologically useful materials. Glass Technol 2003;44:75–81.
[23] Fu H, Fu Q, Zhou N, Huang W, Rahaman MN, Wang D, et al. In vitro evaluation of borate-based bioactive glass scaffolds prepared by a polymer foam replication method. Mater Sci Eng C 2009;29:2275–81.
[24] Liang W, Rahaman MN, Day DE, Marion NW, Riley GC, Mao JJ. Bioactive borate glass scaffold for bone tissue engineering. J Non-Cryst Solids 2008;354:1690–6.
[25] Gorustovich AA, Porto Lopez JM, Guglielmotti MB, Cabrini RL. Biological performance of boron-modified bioactive glass particles implanted in rat tibia bone marrow. Biomed Mater 2006;1:100–5.
[26] Mantsos T, Chatzistavrou X, Roether JA, Hupa L, Arstila H, Boccaccini AR. Non-crystalline composite tissue engineering scaffolds using boron-containing bioactive glass and poly(D, L-lactic acid) coatings. Biomed Mater 2009;4:055002–14.
[27] Liu X, Huang W, Fu H, Yao A, Wang D, Pan H, et al. Bioactive borosilicate glass scaffolds: in vitro degradation and bioactive behaviors. J Mater Sci Mater Med 2009;20:1237–43.
[28] Wu C, Ramaswamy Y, Boughton P, Zreiqat H. Improvement of mechanical and biological properties of porous $CaSiO_3$ scaffolds by poly(D, L-lactic acid) modification. Acta Biomater 2008;4:343–53.
[29] Yunos DM, Bretcanu O, Boccaccini AR. Polymer–bioceramic composites for tissue engineering scaffolds. J Mater Sci 2008;43:4433–42.
[30] Baroli B. From natural bone graft to tissue engineering therapeutics: brainstorming on pharmaceutical formulative requirements and challenges. J Pharm Sci 2009;98:1317–75.
[31] Mouriño V, Boccaccini AR. Bone tissue engineering therapeutics: controlled drug delivery in three-dimensional scaffolds. J R Soc Interface 2010;7:209–27.
[32] Huang D, Zuo Y, Zou Q, Zhang L, Li J, Cheng L, et al. Antibacterial chitosan coating on nano-hydroxyapatite/polyamide66 porous bone scaffold for drug delivery. J Biomater Sci Polym Ed 2011;22:931–44.
[33] Gbureck U, Holzel T, Doillon CJ, Muller FA, Barralet JE. Direct printing of bioceramic implants with spatially localized angiogenic factors. Adv Mater 2007;19:795–800.
[34] Mouriño V, Newby P, Boccaccini AR. Preparation and characterization of gallium releasing 3-D alginate coated 45S5 Bioglass® based scaffolds for bone tissue engineering. Adv Eng Mater 2010;12:B283–91.
[35] Vitale-Brovarone C, Miola M, Balagna C, Verné E. 3D-glass–ceramic scaffolds with antibacterial properties for bone grafting. Chem Eng J 2008;137:129–36.
[36] Brennan EP, Reing J, Chew D, Myers-Irvin JM, Young EJ, Badylak SF. Antibacterial activity within degradation products of biological scaffolds composed of extracellular matrix. Tissue Eng 2006;12:2949–55.
[37] Rowe RC, Sheskey PJ, Quinn ME. Handbook of pharmaceutical excipients. sixth ed. London: The Pharmaceutical Press; 2009.
[38] D'Ayala GG, Malinconico M, Laurienzo P. Marine derived polysaccharides for biomedical applications: chemical modification approaches. Molecules 2008;13:2069–106.
[39] Peters MC, Isenberg BC, Rowley JA, Mooney DJ. Release from alginate enhances the biological activity of vascular endothelial growth factor. J Biomater Sci Polym Ed 1998;9:1267–78.
[40] Hoppe A, Güldal NS, Boccaccini AR. A review of the biological response to ionic dissolution products from bioactive glasses and glass–ceramics. Biomater 2011;32:2757–74.
[41] Barralet J, Gbureck U, Habibovic P, Vorndran E, Gerard C, Doillon CJ. Angiogenesis in calcium phosphate scaffolds by inorganic copper ion release. Tissue Eng A 2009;15:1601–9.
[42] Harris ED. A requirement for copper in angiogenesis. Nutr Rev 2004;62:60–4.
[43] Barbucci R, Lamponi S, Magnani A, Piras FM, Rossi A, Weber E. Role of the Hyal-Cu(II) complex on bovine aortic and lymphatic endothelial cells behavior on microstructured surfaces. Biomacromolecules 2005;6:212–9.
[44] Giavaresi P, Torricelli PM, Fornasari R, Giardino RB, Leone G. Blood vessel formation after soft-tissue implantation of hyaluronan-based hydrogel supplemented with copper ions. Biomater 2005;26:3001–8.
[45] Gérard C, Bordeleau LJ, Barralet J, Doillon CJ. The stimulation of angiogenesis and collagen deposition by copper. Biomater 2010;31:824–31.
[46] Vedel E, Zhang D, Arstila H, Hupa L, Hupa M. Predicting physical and chemical properties of bioactive glasses from chemical composition. Part IV: Tailoring

composition with desired properties. Glass Technol Euro Glass Sci Technol A 2009;50:9–16.
[47] Kokubo T, Huang ZT, Hayashi T, Sakka S, Kitsugi T, Yamamuro T. Ca, P-rich layer formed on high-strength bioactive glass–ceramic A–W. J Biomed Mater Res 1990;24:331–43.
[48] Duarte AR, Mano JF, Reis RL. Preparation of chitosan scaffolds loaded with dexamethasone for tissue engineering applications using supercritical fluid technology. Eur Polym J 2009;45:141–8.
[49] Hollister S. Porous scaffold design for tissue engineering. Nat Mater 2005;4:518–24.
[50] Miao X, Tan LP, Tan LS, Huang X. Porous calcium phosphate ceramics modified with PLGA–bioactive glass. Mater Sci Eng C 2007;27:274–80.
[51] Peroglio M, Gremillard L, Chevalier J, Chazeau L, Gauthier C, Hamaide T. Toughening of bio-ceramics scaffolds by polymer coating. J Euro Ceram Soc 2007;27:2679–85.
[52] Bretcanu O, Misra S, Roy I, Renghini C, Fiori F, Boccaccini AR, et al. In vitro biocompatibility of 45S5 Bioglass®-derived glass-ceramic scaffolds coated with poly(3-hydroxybutyrate). J Tissue Eng Regen Med 2009;3:139–48.
[53] Kuo CK, Ma PX. Ionically crosslinked alginate hydrogels as scaffolds for tissue engineering: Part 1. Structure, gelation rate and mechanical properties. Biomater 2001;22:511–21.
[54] Kuo CK, Ma PX. Maintaining dimensions and mechanical properties of ionicallycrosslinked alginate hydrogel scaffolds in vitro. J Biomater Res A 2008;84:899–907.
[55] Gervais F, Blin A, Massiot D, Coutures JP, Chopinet MH, Naudin F. Infrared reflectivity spectroscopy of silicate glasses. J. Non-Cryst Solids 1987;89:384–401.
[56] Smith BC. Infrared spectral interpretation: a systematic approach. Boca Raton, FL: CRC Press; 1999.
[57] Alsberg E, Kong HJ, Hirano Y, Smith MK, Albeiruti A, Mooney DJ. Regulating bone formation via controlled scaffold degradation. J Dent Res 2003;82:903–8.
[58] Balakrishnan B, Jayakrishnan A. Self-cross-linking biopolymers as injectable in situ forming biodegradable scaffolds. Biomater 2005;26:3941–51.
[59] Bajpai SK, Sharma S. Investigation of swelling/degradation behaviour of alginate beads crosslinked with Ca^{2+} and Ba^{2+} ions. React Funct Polym 2004;59:129–40.
[60] Al-Musa S, Abu Fara D, Badwan AA. Evaluation of parameters involved in preparation and release of drug loaded in crosslinked matrices of alginate. J Controlled Release 1999;57:223–32.
[61] Hong Z, Reis RL, Mano JF. Preparation and in vitro characterization of novel bioactive glass ceramic nanoparticles. J Biomed Mater Res A 2009;88:304–13.
[62] Bouhadir KH, Lee KY, Alsberg E, Damm KL, Anderson KW, Mooney DJ. Degradation of partially oxidized alginate and its potential application for tissue engineering. Biotechnol Prog 2001;17:945–50.
[63] Bhakuni DS, Rawat DS. Bioactive marine natural products. Berlin: Springer Verlag; 2005.
[64] Kim TN, Feng QL, Kim JO, Wu J, Wang H, Chen GC, et al. Antimicrobial effects of metal ions (Ag^{+}, Cu^{2+}, Zn^{2+}) in hydroxyapatite. J Mater Sci Mater Med 1998;9:129–34.
[65] Sutter B, Ming DW, Clearfield A, Hossner LR. Mineralogical and chemical characterization of iron-, manganese-, and copper-containing synthetic hydroxyapatites. J Soil Sci Soc Am 2003;67:1935–42.
[66] Li Y, Ho J, Ooi CP. Antibacterial efficacy and cytotoxicity studies of copper (II) and titanium (IV) substituted hydroxyapatite nanoparticles. Mater Sci Eng C 2010;30:1137–44.
[67] Varmette EA, Nowalk JR, Flick LM, Hall MM. Abrogation of the inflammatory response in LPS-stimulated RAW 264.7 murine macrophages by Zn- and Cu-doped bioactive sol–gel glasses. J Biomed Mater Res A 2009;90(2):317.
[68] Singh RP, Kumar S, Nada R, Prasad R. Evaluation of copper toxicity in isolated human peripheral blood mononuclear cells and it's attenuation by zinc: ex vivo. Mol Cell Biochem 2006;282:13–21.